Atmos. Chem. Phys. Discuss., 8, 12625–12663, 2008
www.atmos-chem-phys-discuss.net/8/12625/2008/

Atmospheric Chemistry and Physics Discussions

Measurements of aerosol absorption and scattering in the Mexico City Metropolitan Area during the MILAGRO field campaign: a comparison of results from the T0 and T1 sites

N. A. Marley[1], J. S. Gaffney[2], T. Castro[3], A. Salcido[4], and J. Frederick[5]

[1]Graduate Institute of Technology, University of Arkansas at Little Rock, Little Rock, AR, USA
[2]Department of Chemistry, University of Arkansas at Little Rock, Little Rock, AR, USA
[3]Centro de Ciencias de la Atmósfera, Universidad Nacional Autónoma de México, México City, México
[4]Instituto de Investigaciones Eléctricas, Gerencia de Sistemas de Calidad Ambiente y Seguridad, Cuernavaca, Morelos, México
[5]Department of Geophysical Sciences, The University of Chicago, Chicago, IL, USA

Received: 29 May 2008 – Accepted: 5 June 2008 – Published: 3 July 2008

Correspondence to: J. S. Gaffney (jsgaffney@ualr.edu)

Published by Copernicus Publications on behalf of the European Geosciences Union.

Abstract

Measurements of aerosol absorption and scattering were obtained in Mexico City during the MILAGRO (Megacity Initiative: Local and Global Research Observations) field campaign in March 2006. A comparison of aerosol absorption and scattering was obtained in Mexico City at site T0 located in the northern part of Mexico City at the Instituto Mexicano del Petróleo Laboratories and at site T1 located at the Universidad Tecnológica de Tecamac, 18 miles northwest of T0. Hourly averages of aerosol absorption were similar at both sites, ranging from 6–93 Mm^{-1} with an average of 31 Mm^{-1} at T0; and from 2–104 Mm^{-1} with an average of 19 Mm^{-1} at T1. Aerosol scattering at T0 ranged from 16–344 Mm^{-1} with an average of 105 Mm^{-1}; while the scattering values at T1 were lower than T0 ranging from 2–136 with an average of 53 Mm^{-1}. Aerosol single scattering albedos (SSAs) were determined at both sites using these data. SSAs at T1 ranged from 0.44–0.90 with an average 0.75 as compared to hose at T0, range 0.51–0.93 with an average of 0.77.

Broadband UV-B intensity was found to be higher at site T0, with an average of 64 $\mu W/cm^2$ at solar noon, than at site T1, which had an average of 54 $\mu W/cm^2$ at solar noon. Comparisons of clear-sky modeled UV-B intensities with the simultaneous UV-B measurements obtained at site T0 and at site T1 for cloudless days indicate a larger diffuse radiation field at site T0 than at site T1. The determination of aerosol scattering Ångstrom coefficient at T0 suggests the larger diffuse radiation is due to the predominance of submicron aerosols at T0 with aerosol scattering of UV-B radiation peaked in the forward direction, leading to the enhancement observed at ground level.

1 Introduction

Megacities, large urban and suburban centers whose populations exceed ten million inhabitants, are steadily increasing worldwide with the most rapid growth in the tropical areas of South America and Asia. In 1800 only 3% of the world's population lived in ur-

ACPD

8, 12625–12663, 2008

ban areas. This increased to 47% by the end of the 20th century. In 1950 there were 83 cities with populations exceeding one million and New York City was the only megacity (UNEP/WHO, 1992). By 2007 there were 468 urban centers of more than one million and of these 14 are classified as megacities with the largest metropolitan complexes centered at Tokyo, Japan, and Mexico City, Mexico (Molina and Molina, 2002). If this trend continues, the world's urban population will double every 38 years and within the next 10 to15 years it is predicted that there will be more than 30 megacities worldwide.

The Mexico City metropolitan area (MCMA) is the largest urban center in North America and the second largest megacity worldwide. It occupies ~3540 km^2 with a population of ~19 million (CAM, 2002). In general, megacities suffer from poor air quality due to the cumulative effects of population growth, industrialization, increased vehicle usage and total energy consumption. However, the topography of the MCMA also acts to exacerbate the poor air quality (Fast et al., 2007; Fast and Zhong, 1998; Doran et al., 1998). Mexico City is located in a basin on the central Mexican plateau at an altitude of 2240 m and latitude of 19° N. The basin is surrounded on the west, south, and east by mountain ranges that rise up to 1000 m above the basin floor. This serves to inhibit dispersion of emissions within the basin and the high levels of incoming solar radiation at this latitude and elevation promotes atmospheric photochemical reactions that rapidly form secondary pollutants (Whiteman et al., 2000).

Due to the elevation and topography of Mexico City, the height of the boundary layer may reach up to 2 km above the surface (Raga et al., 2001a). Therefore, pollutants are emitted from the basin at altitudes that are considered to be free troposphere elsewhere and are expected to travel long distances affecting the surrounding regions (Gaffney and Marley, 1998; Williams et al., 2002). Modeling results have indicated that the effects of this exported pollution can impact background levels up to 200 to 300 km away at 5 km above sea level (Whitemann et al., 2000).

It has been estimated that emissions from the Mexico City basin contribute 15 Megatons of fine aerosol ($PM_{2.5}$) per year to the surrounding regions (Gaffney et al., 1999). This fine aerosol is composed of approximately 55% organic carbon (OC), 11% black

ACPD
8, 12625–12663, 2008

carbon (BC), 10% ammonium nitrate and 20% ammonium sulfate (Chow et al., 2002; Salcedo et al., 2006). The emissions of sulfate aerosols alone from the MCMA are estimated to amount to approximately 1% of the total global sulfate burden (Barth and Church, 1999). While sulfate is well known as an important light scattering aerosol species contributing to atmospheric cooling (Charlson et al., 1992), BC and the associated OC has more recently gained attention as major light absorbing aerosol species exerting a positive radiative forcing and reinforcing the atmospheric warming due to increases in the greenhouse gases (Jacobson 2002; Ramanathan et al., 2005). Some model calculations suggest that the contribution of carbon soot aerosols to global warming may be as much as 0.3–0.4°C, rivaling the contributions from atmospheric methane (Jacobson, 2004; Chung and Seinfeld, 2005). The ultimate climate effects from carbon aerosols will depend on their physical and chemical properties, as well as their residence times and distributions in the atmosphere (Jacobson, 2001).

The presence of the highly absorbing BC aerosols in Mexico City leads to a reduction in overall solar flux of 17.6% locally (Raga et al., 2001b). The mass of these absorbing aerosols exported from this megacity into the surrounding region is estimated to be 6000 metric tons per day or 2 mega-tons per year of BC (Gaffney et al., 1999). Since freshly emitted BC aerosols are hydrophobic, they are expected to be more resistant to washout and have longer lifetimes than more hygroscopic aerosols such as sulfate and nitrate (Gaffney and Marley 2005; Dua et al., 1999). In addition, since in the MCMA these aerosols are introduced into the atmosphere at altitudes that would be considered to be in the free troposphere 300 km away, they are assumed to have longer lifetimes than aerosols released at lower altitudes (Raga et al., 2001b). The MCMA is therefore a major source of BC aerosols to the surrounding regions and the release of these highly absorbing aerosols will have an impact on the radiative balance and climate on a regional scale.

The influences of aerosols on climate are much more complex than those of the greenhouse gasses (Schwartz and Buseck, 2000). Aerosol composition is highly variable, with different species present within the same particle, due to the differ-

ent sources, production mechanisms and atmospheric transformations (Pósfai et al., 1999). In addition, these different aerosol species can be either internally or externally mixed within the particle yielding different optical and microphysical properties and different radiative effects (Pósfai et al., 1999; Schnaiter et al., 2005). Aerosol distributions are also variable both spatially and temporally and although aerosol lifetimes are much shorter than that of the greenhouse gases, estimates range from less than a day to more than a month resulting in transport distances from a few miles to hemispheric scales (Marley et al., 2000; Williams et al., 2002). This variability in properties and distributions make it difficult to quantify the aerosol impacts on climate and to represent these effects in climate models.

In order to better understand the evolution and transport of pollutant aerosols and gases from emissions in the Mexico City basin and their resulting impacts on regional climate, a multiagency field campaign was undertaken called the Megacities Initiative: Local and Global Research Observations (MILAGRO). The MILAGRO study was composed of four collaborative field experiments. Two of the components of the MILAGRO study focused a major part of their efforts on aerosol emissions. The Megacity Aerosol Experiment, Mexico City 2006 (MAX-Mex) was sponsored by the U.S. Department of Energy (DOE) to investigate the direct radiative effect of aerosols in the Mexico City plume as a function of time, location and processing conditions. The MCMA-2006 study, supported by various Mexican institutions, the U.S. National Science Foundation (NSF) and the DOE deployed ground based instrumentation to examine fine particles and secondary aerosol precursor gas emissions within the Mexico City Basin. As part of these two MILAGRO components, aerosol scattering and absorption measurements were obtained at a site located at the Instituto Mexicano del Petróleo (IMP-Mexican Petroleum Institute), in the northwestern part of the Mexico City center. This site, known as T0, was chosen to represent the fresh emissions within the MCMA. Measurements were also obtained at the Universidad Tecnológica de Tecamac (Technological University of Tecamac), located approximately 29 km (18 mi) northwest of T0. This site, known as T1, was expected to represent a mixture of both fresh and aged

ACPD
8, 12625–12663, 2008

pollutants as they exit the basin.

The evolution of absorbing aerosols downwind of Mexico City has been described previously in a comparison of measurements obtained at site T1 with those obtained at site T2 (Rancho La Bisnaga), located approximately 35 km (22 mi) north-northeast of T1 (Doran et al., 2007, 2008; Doran, 2007). This study focused primarily on the changes in BC, also known as elemental carbon (EC), and OC content of the aerosols and the resulting effects on the aerosol mass specific absorption coefficients. It was concluded from this work that emission sources outside the MCMA, including biomass-burning sources, are important contributors to the regional aerosol burden.

Presented here is a comparison of measurements of aerosol absorption and aerosol scattering obtained at sites T0 and T1 during the MILAGRO campaign. In addition, mass specific aerosol absorption coefficients were determined with total carbon measurements taken from high-volume quartz filters and these are compared with values reported in the previous study of (Doran, et al., 2007). These data are used to estimate the distribution and evolution of aerosol optical properties within the surrounding region of the Mexico City basin. Also reported here is a comparison of UV-B radiation measurements obtained simultaneously at sites T0 and T1, under cloudless conditions, with clear sky modeled UV-B values. These are discussed with regard to the light scattering measurements obtained at both sites.

2 Experimental methods

2.1 Sample sites

2.1.1 Site T0

Measurements were obtained from March 10 (day 69) to March 29 (day 88), 2006 at the Instituto Mexicano del Petróleo (IMP) laboratories [Mexico, D. F.]. This site, known as T0, is located in the north central part of Mexico City at latitude 19° 29′ N, longitude

99° 09′ W, and at an altitude of 2240 m above sea level. The IMP complex is a campus of 33 buildings located in an industrial and commercial area of Mexico City surrounded by streets that are very heavily trafficked by light duty vehicles and diesel buses. The nearest major roads are approximately 300 m away from the measurement site.

2.1.2 Site T1

Measurements were also obtained from March 1 (day 60) to 29 March (day 88), 2006 at the Technological University of Tecamac, State of Mexico, 30 km (18 mi) north of Mexico City. This site, known as T1, is at latitude 19° 43′N and longitude 98°58′W at an altitude of 2340 m above sea level. Tecamac County is bordered on the north by the State of Hidalgo and on the west by Teotihuacan. The prevailing climate in the region is temperate, semi-dry with frequent summer rains. It has an annual average precipitation of 636 mm. Medium annual temperature is 16.4 °C with a maximum of 31.5°C and a minimum of 6.5°C. Tecamac has a recorded population of 172,410, as of the 2000 census, and is primarily commercial with 1923 food businesses, 1147 other businesses and 9 markets. The principal mode of transportation in the area consists of light duty vehicles, and small diesel buses. The main transportation route is the public road # 85, which runs south to north through the area from Mexico City to Pachuca. The municipality of Pachuca, which is located 94 km (58 mi) northeast of Mexico City and 64 km (40 mi) northeast of Tecamac, is the capital of the state of Hidalgo with a recorded population of 267 751 in 2005. Numerous industries are based in the surrounding areas, including automobile parts, ovenware, tools and mining equipment. During most of the year there are strong northeasterly winds that can reach 46 mph.

ACPD
8, 12625–12663, 2008

2.1.3 Aerosol optical properties

2.1.4 Site T0

Aerosol instrumentation at site T0 was located on the rooftop of Building No. 32 (Héctor Lara Sosa Building, IMP) 15 m above ground level. The sample inlets were designed to collect aerosols in the 0.1 to 2 micron size range. Aerosol scattering was measured with a three wavelength integrating nephelometer (TSI Model 3563) operating at 450, 530, and 660 nm. Results obtained at 530 nm are reported here. An internal high efficiency particulate filter (HEPA) is used to provide a clean air measurement periodically for background subtraction. The TSI nephelometer was operated at ambient relative humidity. However, two single wavelength nephelometers (Meteorology Research Incorporated) were operated at low (20%) and high (95%) relative humidity for comparison.

Aerosol absorption was measured with a multi-angle absorption photometer, or MAAP (Thermo Electron Model 5012). The aerosols in the air sample are collected within the instrument by continuous filtration through a glass fiber tape strip. As the sample is deposited on the filter tape, the light attenuation steadily increases. At high sample loadings the high absorption can cause detection limits to decrease. To prevent this, the instrument automatically advances the tape to a new sample spot when light attenuation reaches 25% of its initial value. After the tape advance, a background measurement is taken to correct for variations in filter surfaces and source light intensities.

The instrument uses a multiple detector setup to simultaneously measure the 670 nm light intensity both transmitted and scattered from the particle-loaded filter tape. The instrument then uses a two-stream-approximation radiative transfer scheme to determine aerosol absorption. This explicit treatment of light scattering effects caused by the aerosol and filter matrix in the radiative transfer scheme improves the determination of aerosol absorption considerably over methods that rely on the measurement of transmission or reflection alone (Petzold et al., 2005).

ACPD
8, 12625–12663, 2008

The instrument automatically calculates the BC content in the aerosol samples from the aerosol absorption measurements by assuming BC to be the main absorbing aerosol species in the samples with a mass specific absorption coefficient of 6.6 m^2/g at 670 nm. However, these results are easily reconverted to the initial aerosol absorption measurement using the manufacturer's absorption coefficient. The analog outputs of the absorption photometer and the nephelometers were monitored continuously and one-minute averages of aerosol absorption and scattering were recorded by a laptop computer operating with LabVIEW software. These data are reported here as an hourly running average of the one minute values.

2.1.5 Site T1

The sample inlet at site T1was located at a height of 10 m above ground level and collected aerosols in the 0.1 to 2 micron size range at a flow rate of 16.7 l/min at ambient temperature and pressure. Aerosol absorption was obtained by a particle soot absorption photometer or PSAP (Radiance Research). This method is also a filter based measurement technique. The particle laden air stream is first passed through a primary filter and the change in light intensity from a 567 nm LED is measured to determine aerosol absorption. The clean air stream is then passed through a second filter adjacent to the primary filter. This second filter is used as a reference in order to ensure that the observed change in primary filter transmittance is not due to changes in the intensity of the LED light source.

Corrections were made to the absorption measurements to account for the magnification of the absorption by the filter medium and for nonlinearities in the response of the instrument as the filter is loaded with particulates. These correction factors have been determined empirically by the manufacturer to be

$$\sigma_a = (\sigma_{meas} - K_1\sigma_s)/K_2 \quad (1)$$

where σ_a is the corrected aerosol absorbance, σ_{meas} is the measured aerosol absorbance, σ_s is the measured aerosol scattering, K_1=0.02, and K_2=1.2 (Bond et al.,

1999). In addition, transmittance values below 0.5 have been omitted as invalid due to low particle loadings on the filter.

Forty-six minute averages of aerosol absorption obtained from day 74 through day 85 with a photoacoustic spectrometer operating at 880 nm have been reported previously for site T1 (Doran et al., 2007). These absorption values varied from 1–50 Mm^{-1} while the absorption values obtained by the PSAP at 567 nm varied from 14–114 Mm^{-1}. The daily maximum absorbance values obtained by the PSAP exceed the maximum values reported by Doran et al. (2007) by approximately 60% over the same time period. This difference is due to the different wavelengths used to obtain the measurements. The absorption of light by fine aerosol particles (A) is generally thought to be broadband with a wavelength dependence defined for any wavelength range (λ_1, λ_2) by the absorption Ångstrom coefficient (α_A) where

$$A = \beta\lambda^{-\alpha} \text{ and} \quad (2)$$

$$\alpha_A(\lambda_1, \lambda_2) = -\ln(A_1/A_2)/\ln(\lambda_1/\lambda_2). \quad (3)$$

For small spherical particles with a constant refractive index across the wavelength range λ_1, λ_2, α_A=−1 (Bergstrom, 1973). This has been determined to be a good approximation for aerosols composed mostly of BC or for particles containing a significant fraction of OC over a narrow wavelength range <600 nm (Bergstrom et al., 2002; Kirchstetter et al., 2004).

The wavelength dependence of absorption by mixed carbon aerosols in the Amazon Basin containing BC, secondary OC, and primary OC from biomass burning has been found to be closer to −1.5 (Schmid et al., 2006). In addition, aerosol absorption measured in areas impacted heavily by biomass burning exhibited a wavelength dependence of −2 to −2.5 (Dubovik et al., 1998; Kirchstetter et al., 2004; Swap et al., 2003). During much of the MILAGRO study, site T1 was impacted by local grass fires, which could have contributed significantly to the overall aerosol loadings and to an enhanced wavelength dependence of the aerosol absorption. This is confirmed by

ACPD
8, 12625–12663, 2008

^{14}C analysis of 12-h aerosol samples collected at site T1, which found that 70% of the carbon in the aerosols was from modern sources (Gaffney et al., 2008).

A comparison of the daily absorbance maxima reported at 880 nm (Doran et al., 2007) with those recorded by the PSAP at 560 nm using Eq. (3) yields a wavelength dependence of aerosol absorption of −2.1 at site T1. This is consistent with the previous results reported for aerosols impacted by biomass burning. If the value of $\alpha_A = -2.1$ is used to correct both the PSAP and the photoacoustic data to 670 nm, the differences in the results are reduced to an average of 7% which is well within the expected instrumental error of the PSAP (Bond et al., 1999). The PSAP results reported here for site T1 are corrected to 670 nm by using Eq. (3) with $\alpha_A = -2.1$ in order to provide a direct comparison with the MAAP measurements obtained at site T0.

Aerosol scattering was measured at site T1 with a portable integrating nephelometer (Radiance Research Model 903) operating at 530 nm. The measurements were recorded by internal data loggers at 1 min intervals. The stored data was retrieved using a personal computer through an RS232 port. These data are reported here as an hourly running average of these one minute values.

2.2 Meteorology and UV-B measurements

Broadband ultraviolet-B (UV-B) radiation measurements were taken at both site T0 and site T1 with Robertson-Berger (RB) radiometers (Solar Light Co. Model 501). These radiometers record continuous measurement of global (direct+diffuse) broadband ultraviolet radiation from 280–320 nm. Since the output of the detectors vary 1% per degree C, the internal temperatures of the radiometers are maintained at 25±1°C with Peltier elements inside the housings. Both radiometers were factory calibrated with a 200 W quartz halogen lamp traceable to NIST. The detector has a spectral response that mirrors the erythemal action spectra (Mckinlay and Diffey, 1987). They are calibrated in units of minimum erythemal dose per hour (MED/hr) where one MED/hr is defined as 0.0583 W/m^2.

ACPD
8, 12625–12663, 2008

Measurements of wind speed, wind direction, rain intensity, pressure, temperature, and relative humidity (RH) were obtained at both sites with weather multi-sensor packages (Vaisala, WXT150). Rain intensity measurements reported here were made by the RAINCAP sensor included in the weather package. The sensor detects the impact of individual raindrops by a piezoelectric sensor. The resulting voltage signal is proportional to the volume of the drop and is converted into total accumulated precipitation. All measurements were collected at a one-minute time resolution with a laptop computer operating with LabVIEW software.

2.3 Total carbon determinations

Samples of fine (<1.0 micron) aerosols were collected in Mexico City from 1 March (day 60) to 28 March (day 68), 2006 at site T0 and site T1. The Aerosol samples were collected on quartz fiber filters by using high volume samplers (Hi-Q Environmental. Products, Model HVP-3800AFC) equipped with cascade impactors (Thermo Anderson). The air samplers were equipped with brushless, three stage centrifugal fan blowers controlled by an electronic mass flow sensor that detects changes in the operators pre-set flow rate caused by changes in temperature, barometric pressure, and pressure drop due to particulate loading on filter media. The high-volume sampler compensates for these changes by adjusting the motor speed to maintain the pre-set flow rate at 40 scfm. Three separate LCD's, display elapsed time, total volume of air sampled, and instantaneous flow rate. The quartz filter samples were taken at 12-h intervals from 05:30 to 17:30 and from 17:30 to 05:30 local standard time (LST). The volume of air sampled during the 12-h time period averaged 740 m^3 with an average aerosol loading of 13 mg total carbon content. The 0.1 to 1.0 micron quartz filter aerosol samples were analyzed for total carbon content by high temperature combustion followed by measurement of evolved carbon dioxide.

ACPD
8, 12625–12663, 2008

3 Results and discussion

The results of fine aerosol absorption and scattering at sites T0 and T1 are shown in Fig. 1. Aerosol absorption at site T0 ranged from 6–93 Mm^{-1} with an average of 31 Mm^{-1} and followed a diurnal pattern that reached a maximum at around 06:30 (range of 05:00 to 08:00) LST and a minimum at 13:00 (range of 12:00 to 14:00) LST. These values can be compared to aerosol absorption measurements obtained in Santiago, Chile, which has a similar terrain but lower altitude. The major sources of absorbing aerosols in both Mexico City and Santiago are motor vehicle traffic, especially diesel buses (Horvath et al., 1997; Molina and Molina, 2002). Aerosol absorption in Santiago was found to reach maximum values of 100–200 Mm^{-1} at around 09:00 LST and correlated with peak traffic hours (Horvath et al., 1997).

Aerosol absorption measurements at site T1 ranged from 2–104 Mm^{-1} with an average of 19 Mm^{-1}. The same diurnal pattern observed at T0 was also evident at site T1 (maximum at 06:30 and minimum at 13:00 LST). While the daily maximum absorption values at T1 exceeded those at T0 on 6 of the days studied, these high levels were of much shorter duration, lasting only about 1 to 2 h as compared to 7 to 9 h of peak levels at site T0. In addition, the minimum aerosol absorption levels at site T1 routinely fell below the minimum values observed at site T0.

Aerosol scattering measurements obtained at site T0 ranged from 16–344 Mm^{-1} with an average of 105 Mm^{-1}. Scattering values generally reached a maximum at 10:30 (range of 07:30 to 13:00) LST. Measurements of aerosol scattering species obtained in Mexico City in April 2003 found that both nitrate and ammonium concentrations showed a sharp diurnal pattern with a maximum of 10–20 $\mu g/m^3$ for nitrate and 4–8 $\mu g/m^3$ for ammonium occurring from 10:00–12:00 LST, while sulfate concentrations did not vary significantly, remaining at round 2–3 $\mu g/m^3$ most of the time (Salcedo et al., 2006). The sharp diurnal pattern of nitrate is due to the photochemical formation of nitric acid from the reaction of NO_2 and OH, and subsequent reaction with ammonia to form the highly scattering aerosol species ammonium nitrate. This late morning formation of

ACPD
8, 12625–12663, 2008

ammonium nitrate in Mexico City gives the aerosol scattering the diurnal profile shown in Fig. 1.

Aerosol scattering measured in Denver during the winter reached a maximum of 60–140 Mm^{-1} at approximately 14:00–19:00 LST (Groblickiet al., 1981). The primary aerosol scattering species in Denver is ammonium sulfate formed from the atmospheric oxidation of SO_2, with significant contributions from ammonium nitrate, as well. The photochemical formation of these secondary aerosol species would be expected to be slower in Denver due to the lower actinic flux in the winter at higher latitudes.

Aerosol scattering values at T1 were in general much lower than at T0, ranging from 2–136 Mm^{-1} with an average of 53 Mm^{-1}, reaching a maximum at 08:30 (range of 06:00 to 13:30) LST. On clear days the boundary layer in Mexico City during March–April grows slowly after sunrise at 06:40 to a height of approximately 1000 m by 11:00 LST (Doran et al., 1998, 2007). This serves to dilute the pollutants already present in the boundary layer. After 12:00 LST the boundary layer grows rapidly to 3000 m or greater. The maximum scattering values at site T0 occurred 2 h later than the maximum scattering values seen at T1 and 4 h later than the peak aerosol absorption values. This suggests that the high aerosol scattering values measured at T0 were primarily due to rapid secondary aerosol formation in the city. The values for aerosol scattering at T1 were controlled primarily by changes in the boundary layer height in the early morning, and by the presence of photochemically aged aerosols in the afternoon (Carabalì, 2008).

The single scattering albedo (SSA) is defined as the ratio of aerosol scattering to total light extinction (absorption + scattering) as

$$\mathrm{SSA} = \sigma_s/(\sigma_s + \sigma_a) \quad (4)$$

where σ_s is the aerosol scattering coefficient and σ_a is aerosol absorption coefficient The SSA is therefore the fraction of total light extinction that is due to scattering by aerosols. The SSA is a function of aerosol chemical composition and morphology. For a completely scattering aerosol, such as sulfate, the SSA ~1 and for a completely

ACPD
8, 12625–12663, 2008

absorbing aerosol, such as freshly emitted BC, the SSA ~0. The aerosol SSAs calculated from the ground level absorption and scattering measurements at T0 and T1 are shown in Fig. 2. The lower aerosol scattering observed at site T1 translates into lower values for aerosol SSA at T1 with a range of 0.44–0.90 and an average of 0.75 the very low values for SSA at T1 are of very short duration. The aerosol SSA determined at T0 of 0.51–0.93 with an average of 0.77. While the SSAs recorded over most of the Northern Hemisphere are about 0.85–0.95 (Jacobson, 2001), recently values as low as 0.68 have been reported over the southern Atlantic Ocean (Clark, 1989). Aerosols with an SSA>0.95 will have a negative climate forcing and an overall cooling effect on the atmosphere, while an SSA<0.85 will result in a positive climate forcing and an overall warming effect due to the enhanced aerosol absorption (Ramanathan et al., 2001).

Doran et al. (2007) have calculated forward and back trajectories of air masses at 1000 m above ground level (AGL) over site T1 during daylight hours (06:00–18:00 LST) for a 20-day period during the month of March 2006 (Doran et al., 2007). The most favorable conditions for transport from site T0 to site T1 were seen to occur on days 69, 70, 77, 78, 79, 81, 83, 86 and 87. On days 71–76 and day 82 the trajectories indicate that transport would have likely been from site T1 towards Mexico City and site T0. The aerosol absorption, scattering, and SSAs obtained at site T0 and T1 have been averaged over the same daylight hours for direct comparison to the back trajectories reported by Doran et al. (2007).

The daily average aerosol absorption at sites T0 and T1 is shown in Fig. 3 along with the measurement ranges observed during each day. The daily average absorption values are similar at both sites ranging from 14–44 Mm^{-1} with an overall average value of 31 Mm^{-1} at T0 and a range of 13–35 Mm^{-1} with an overall average of 25 at site T1. The two sites differ primarily in the range of aerosol absorption values observed during the day. While the lower limits on the ranges are similar at both sites, indicating a regional background of 5–10 Mm^{-1}, the upper limits of the aerosol absorption measurements are more variable at site T1 with a range of 15–114 Mm^{-1} as compared to site T0 with a range of 40–83 Mm^{-1}. There also appears to be no clear correlation

of absorption values with transport from the Mexico City area, again indicating a local source of absorbing aerosols at site T1. Days 77, 86 and 87, which were identified as likely transport days from site T0 to site T1, show high maximum aerosol absorbance. However, high maxima were also observed on days when transport has been identified as from the north (72 and 74). This suggests an impact at site T1 from Tizayuca (an important industrial center) and Pachuca, which are located 10 and 64 km northeast of T1.

Total carbon concentrations (TC) obtained on aerosol samples collected over the daylight hours at sites T0 and T1 are shown in Fig. 4. The overall profile of the daily carbon concentrations during the study period is similar at both sites with higher values during the first part of the study (25–35 $\mu g/m^3$) and lower values (5–15 $\mu g/m^3$) during the latter part of the study. The TC results were used to calculate the average aerosol mass absorption coefficients at 670 nm from the absorbance values in Fig. 3. The mass absorption coefficients for TC aerosols at 670 nm, shown in Fig. 5 (top), were similar at both sites ranging from 1–3.1 m^2/g with an average of 2 m^2/g. While the mass absorption coefficient of freshly emitted BC aerosols is estimated to be in the range of 6.3–8.7 m^2/g at 550 nm (Bond and Bergstrom, 2006), OC aerosol species such as humic like substances (HULIS) derived from biomass burning or secondary organic aerosols generated photochemically have mass absorption coefficients <1 m^2/g at 550 nm (Hoffer et al., 2006; Patterson and McMahon, 1984). The overall mass absorption coefficients measured for total carbon (BC+OC) will be dependent on the relative concentrations of BC and OC as well as their mixing state (Hitzenberger and Pauxbaum, 1993; Bond et al., 2006). The similarity of the TC mass absorption for both sites T0 and T1 suggests that the aerosol carbon composition was similar at both sites.

Mass absorption coefficients for BC were calculated assuming that the total carbon content of the <0.1 micron aerosols was 30% BC. This is in good agreement with past measurements made in the Mexico City area (Chow et al., 2002) as well as for measurements made in other urban areas (Tanner et al., 1982; Gaffney et al., 1984). The

adjusted values reported for OC/EC ratios measured at site T1 are also in this range (Doran, 2007). The BC mass absorption coefficients range from 4.2–10.7 m^2/g with an average of 7.0 m^2/g at T0 and from 4.7–10.4 m^2/g with an average of 6.7 m^2/g at T1. The median values of the mass absorption for EC reported for T1 by continuous OC/EC analysis were 5.6 m^2/g at 880 nm (Doran, 2007). This would correspond to a mass absorption coefficient of 7.3 m^2/g at 670 nm assuming a λ^{-1} absorption dependence for BC.

The aerosol scattering averaged over the daylight hours is shown in Fig. 6 for sites T0 and T1 along with the measurement ranges for each day. The daily averages vary from 62–197 Mm^{-1} with an overall average of 125 Mm^{-1} at T0. The daily average aerosol scattering was lower and more consistent at site T1 with a range of 38–105 Mm^{-1} and an overall average of 57 Mm^{-1}. There also does not seem to be a general trend of major impacts on aerosol scattering at T1 due to transport from Mexico City except for possibly day 81. Day 81 was identified as having favorable conditions for transport from site T0 to site T1 (Doran et al., 2007) and that day showed high scattering values for both sites.

The period from day 82 to day 87 was dominated by heavy regional rains and an overall increase in relative humidity (see Fig. 7). Rain totals before day 82 were 0 mm at site T0 and 6.7 mm at site T1. After day 82 rain totals were 19.2 mm at T0 and 59.5 at T1. This was accompanied by an increase in the average daily maximum RH from 59% to 76% at T0 and from 73% to 89% at T1. The increased rains resulted in a decrease in aerosol scattering at both sites by approximately the same amount. The average aerosol scattering at site T0 before the rainy period was 128 Mm^{-1} (range of 62–197 Mm^{-1}) and during the rainy period the aerosol scattering dropped to 118 Mm^{-1} (range of 85–157 Mm^{-1}). The same values for site T1 were 61 Mm^{-1} (range of 39–105 Mm^{-1}) before day 82 and 50 Mm^{-1} (range of 38–66 Mm^{-1}) after day 82. However, the aerosol absorption remained the same at site T0 with a value before day 82 of 31 Mm^{-1} (range of 14–44 Mm^{-1}) and a value of 31 Mm^{-1} (range of 19–36 Mm^{-1}) after day 82. The aerosol absorption at T1 decreased slightly from 26 Mm^{-1} (range of 16–

ACPD
8, 12625–12663, 2008

35 Mm^{-1}) before the rainy period to 22 Mm^{-1} (range of 13–32 Mm^{-1}) during the rainy period. Since scattering aerosols are primarily inorganic and hydrophilic, it is expected that they will wash out more readily during rain events than the freshly emitted absorbing BC aerosols that are more hydrophobic in nature (Marley et al., 2000; Gaffney and Marley, 2005; Marley and Gaffney, 2007). However, as the BC aerosols become coated with secondary aerosol species, they will become more hydrophilic in nature and their washout rates would be expected to increase.

The daily average aerosol SSAs at site T0 and T1 are shown in Fig. 8. The average SSA at site T0 ranged from 0.74–0.85 with an overall average of 0.80 while the average SSA at T1 was slightly lower and ranged from 0.71–0.84 with an overall average of 0.76. The aerosol daily SSAs show only a small change at site T0 any change due to the increase in rain intensity, with 0.80 (range 0.76–0.85) prior to day 82 and 0.79 (range 0.74–0.85) after day 82. The corresponding values for site T1 were 0.76 (range 0.71–0.84) prior to day 82 and 0.76 (range 0.75–0.80) after day 82.

Doran et al. (2007) reported daily average aerosol SSAs at T1 determined from MFRSR data at 500 nm on days 71, 78 and 86 as 0.84, 0.85 and 0.89 (Doran et al., 2007). The corresponding average SSA reported here are 0.76, 0.79, and 0.75 as determined from ground-based aerosol absorbance and scattering measurements. The differences in the reported values arise from the differences in measurement methods. The MFRSR values yield a total column measurement that includes all particles present in the atmosphere, while the values calculated in this work represent a surface measurement of fine aerosol particles only. The fine aerosol fraction measured here (0.1 to 2 micron) is more highly absorbing than the much larger mineral dust particles (>2 micron), which are included in the MFRSR measurements and are excellent scatterers. In addition, the aerosol SSAs are also a function of wavelength and the relative values at 500 nm and 670 nm will depend on both the aerosol absorption Ångstrom coefficient (Eq. 3) and the aerosol scattering Ångstrom coefficient (see Eq. 5).

Daily average aerosol SSAs have also been reported for La Merced, located in central Mexico City, and Pedregal, a suburban neighborhood in the southwest portion of

ACPD
8, 12625–12663, 2008

Mexico City during March of 1997 (Eidels-Dubovoi, 2002). These SSA values were calculated from ground level aerosol absorption measurements obtained with a single channel aethalometer and aerosol scattering measurements obtained by an open air integrating nephelometer. The SSA values reported at La Merced varied from 0.63–0.86 with an average of 0.72 and those reported at Pedregal ranged from 0.60–0.84 with an average of 0.68.

Broadband UV-B measurements obtained at sites T0 and T1 are shown in Fig. 9. The UV-B intensity was higher at site T0, with an average of 64 μW/cm^2 and a range of 50–70 μW/cm^2 at solar noon, than at site T1, which had an average of 54 μW/cm^2 and a range of 48–58 μW/cm^2 at solar noon. In general, UV-B reached a maximum at both sites at 12:30 LST. However, the variability of the daily maximum was larger at site T0 (11:30–14:00 LST) than at site T1 (12:00–13:00 LST). A comparison of simultaneous measurements from site T0 and T1 for cloudless days gave a correlation coefficient of 0.931 (slope of 1.18, intercept of 1.01). The measured UV-B irradiances have been compared to that expected for clear sky conditions as determined by a radiative transfer model developed at The University of Chicago (Frederick and Lubin, 1988). The input to this model includes column ozone, determined from TOMS data, atmospheric optical thickness, UV-B surface albedo, site location, day of year and time of day. The results of this comparison are shown in Fig. 10 for days without rain events. Note that both sites show reduced UV-B radiation (i.e. less than the clear sky modeled values) as expected for sites with significant UVB absorbing gases and BC from diesel and biomass burning. The reduction in UV-B has been reported in previous field studies where smoke events have impacted Phoenix, AZ (Gaffney et al., 2002).

The measured UV-B at both sites showed good correlation with the modeled UV-B values (r^2=0.95, 0.96). However, the slope for site T0 was 0.87 while that for site T1 was 0.72. The ratio of UV-B measurements obtained simultaneously at site T0 and site T1 for cloudless days are shown in Fig. 11 as a function of solar zenith angle (SZA). This ratio of measured UV-B at T0 to UV-B at T1 increases dramatically at high SZAs. At high SZAs, when the sun is close to the horizon, the optical path is sufficiently long

ACPD
8, 12625–12663, 2008

that the majority of radiation measured by the RB meters is from the diffuse radiation field. The ratio of direct to diffuse insolation measured by the RB meter is 1.3 at a SZA of 20 deg. and reaches 0.1 at an SZA of 70° (Granger et al., 1993). Therefore, the data shown in Fig. 11 suggests that the diffuse radiation field at site T0 is much larger than that at site T1.

The aerosol scattering values (σ_s) measured by the three wavelength nephelometer located at site T0 have been used to calculate the average aerosol scattering Ångstrom coefficient (α_S) as:

$$\alpha_S = -[\ln \sigma_s\,(450\,\text{nm})/\ln \sigma_s(700\,\text{nm})]/[\ln(700)/\ln(450)]. \quad (5)$$

The Ångstrom coefficient for aerosol scattering is related to the particle size distribution with higher values (α_S>1) typically observed for accumulation mode particles (0.1–1.0 micron) and lower values (α_S≈0) for coarse mode particles (Hand et al., 2004). The values calculated for site T0 ranged from 0.93 to 1.30 with an average of 1.11 over the entire study period. This corresponds to an average effective particle radius of 0.3 micron. (O'Neill and Royer, 1993; Lenoble and Brogniez, 1985). In addition, the Ångstrom scattering exponent of 1.1 corresponds to a scattering asymmetry factor of 0.7 (Lenoble and Brogniez, 1985), which implies that the aerosol scattering intensity will be peaked in the forward direction (45°). Therefore, the predominance of highly scattering submicron aerosols at T0 results in a larger amount of diffusely scattered radiation and a higher UV-B intensity at ground level than seen at site T1.

4 Conclusions

Measurements of aerosol absorption and scattering were obtained in Mexico City at site T0 located in the northern part of Mexico City at the IMP (Instituto Mexicano del Petróleo) laboratories and for site T1 located at the Technical University of Tecamac, 18 miles northwest of T0. Hourly averages of aerosol absorption were similar at both sites, ranging from 6–93 Mm^{-1} with an average of 31 Mm^{-1} at T0 and from 2–104 with

ACPD
8, 12625–12663, 2008

an average of 19 Mm^{-1} at T1. Aerosol scattering at T0 ranged from 16–344 with an average of 105 Mm^{-1} while the scattering values at T1 were in general much lower ranging from 2–136 with an average of 53 Mm^{-1}. The maximum scattering values at site T0 occurred 2 h later than the maximum scattering values seen at T1 and 4 h later than the peak aerosol absorption values at either site. This suggests that the high aerosol scattering values measured at T0 were primarily due to rapid secondary aerosol formation in the city, while the values at T1 were controlled primarily by changes in the boundary layer height in the early morning. The lower aerosol scattering values result in lower values for aerosol SSA at T1 with a range of 0.44–0.90 and an average of 0.75 compared to that at T0 of 0.51–0.93 with an average of 0.77.

Comparisons of aerosol absorption averaged over the daylight hours with back trajectories reported by Doran et al. (2007) showed no clear correlation with transport from the Mexico City area, indicating a local source of absorbing aerosols at site T1, as suggested earlier (Doran et al., 2007). Similar comparisons of scattering measurements averaged over the daylight hours also does not seem to show a general trend of major effects on aerosol scattering at T1 due to transport from Mexico City except for possibly day 81. Day 81 was identified as having favorable conditions for transport from site T0 to site T1 (Doran et al., 2007) and that day showed high scattering values for both sites.

Broadband UV-B intensity was higher at site T0, with an average of 64 $\mu W/cm^2$ and a range of 50–70 $\mu W/cm^2$ at solar noon, than at site T1, which had an average of 54 $\mu W/cm^2$and a range of 48–58 $\mu W/cm^2$ at solar noon. Comparisons of modeled UV-B intensities with the simultaneous UV-B measurements obtained at site T0 and at site T1 for cloudless days imply a larger diffuse radiation field at site T0 than at site T1. The determination of aerosol scattering Ångstrom coefficients at T0 suggests the predominance of submicron aerosols at T0 with aerosol scattering peaked in the forward direction leading to the enhanced diffuse radiation at T0. This enhanced UV-B diffuse radiation would help to explain the significant photochemistry observed in the Mexico City area during MILAGRO, despite the reduction in UVB anticipated from light

ACPD
8, 12625–12663, 2008

absorbing species.

The results of this study confirm that the megacity environments have significantly lower SSAs due to the high concentrations of absorbing carbonaceous aerosols. The common occurrence of SSAs <0.85 will result in a positive climate forcing and an overall warming effect (Ramanathan et al., 2001) which will contribute to the urban heat island effects in these megacities. As well, the BC from fossil emissions in the urban environment along with biomass burning contributions in the region also lead to significant aerosol absorption which will lead to local warming in the boundary layer at both the urban and regional sites. This may help to explain the rapid increase in the boundary layer height observed in past studies in this area and would indicate that studies of boundary layer meteorology processes need to consider absorbing aerosol species when calculating heating rates (Fast and Zhong, 1998; Whiteman et al., 2000).

Acknowledgements. This work was conducted as part of the Department of Energy's Atmospheric Science Program as part of the Megacity Aerosol Experiment – Mexico City, and as part of the MCMA2006 study during MILAGRO. This research was supported by the Office of Science (BER), U.S. Department of Energy Grant No. DE-FG02-07ER64329 and the Mexican Government through SEMARNAT (FOSEMARNAT-2004-01-116) and the Metropolitan Environmental Commission. We wish to thank Mr. Rick Petty and Ashley Willamson of OBER for their continuing encouragement. We also wish to thank Mexican scientists and students from the Instituto Mexicano del Petróleo (IMP) and CENICA, for their assistance, and also to M. I. Saavedra from CCA, UNAM. Thanks also to Neil Sturchio, Ms. Linnea Heraty, and Ms. Nancy Martinez of the University of Illinois at Chicago for their assistance in obtaining TC measurements reported here, and to Luisa Molina and Sasha Madronich for their organizational assistance with MILAGRO.

References

Barth, M. C. and Church, A. T.: Regional and global distributions and lifetimes of sulfate aerosols from Mexico City and southeast China, J. Geophys. Res., 104, 30 231–30 239, 1999.

Bergstrom, R. W.: Extinction and absorption coefficients of the atmospheric aerosol as a function of particle size, Beitraege zur Physik der Atmosphaere, 46, 223–234, 1973.
Bergstrom, R. W., Russell, P. B., and Hignett, P.: Wavelength dependence of the absorption of black carbon particles: Predictions and results from the TARFOX experiment and implications for the aerosol single scattering albedo, J. Atmos. Sci., 59, 567–577, 2002.
Bond, T. C., Anderson, T. L., and Campbell, D.: Calibration and intercomparison of filter-based measurements of visible light absorption by aerosols, Aerosol Sci. Technol., 30, 582–600, 1999.
Bond, T. C. and Bergstrom, R. W.: Light absorption by carbonaceous particles: An investigative review, Aerosol Sci. Technol., 40, 27–67, 2006.
Bond, T. C., Habib, G., and Bergstrom, R. W.: Limitations in the enhancement of visible light absorption due to mixing state, J. Geophys. Res., 111, D20211, doi:10.1029/2006JD007315, 2006.
CAM: Programa para Mejorar la Calidad del aire de la Zona Metropolitana del Valle de Mexico 2002–2010, 2002.
Carabalí, G.: Caracterización morfológica, óptica y química de partículas muestreadas en el sitio T1 de la campaña MILAGRO. Tesis de Maestría, Universidad Nacional Autónoma de México, México, 2008.
Charlson, R. J., Schwartz, S. E., Hales, J. M, Cess, R. D., Coakley, Jr., J. A., Hansen, J. E., and Hoffman, D. J.: Climate forcing by anthropogenic aerosols, Science, 255, 423–430, 1992.
Chow, J. C., Watson, J. G., Edgerton, S. A., and Vega, E.: Chemical composition of $PM_{2.5}$ and PM_{10} in Mexico City during winter 1997, Sci. Total Environ., 287, 177–201, 2002.
Chung, S. H. and Seinfeld, J. H.: Climate response of direct radiative forcing of anthropogenic black carbon, J. Geophys. Res., 110, D11102, doi:10.1029/2004JD005441, 2005.
Clark, A. D.: Aerosol light absorption by soot in remote environments, Aerosol Sci. Technol. 10, 161–171, 1989.
Doran, J. C., Abbott, S., Archuleta, J., Bian, X., Chow, J., Coulter, R. L., de Wekker, S. F. J., Edgerton, S., Elliott, S., Fernandez, A., Fast, J. D., Hubbe, J. M., King, C., Langley, D., Leach, J., Lee, J. T., Martin, T. J., Martinez, D., Martinez, J. L., Mercado, G., Mora, V., Mulhearn, M., Pena, J. L., Petty, R., Porch, W., Russell, C., Salas, R., Shannon, J. D., Shaw, W. J., Sosa, G., Tellier, L., Templeman, B., Watson, J. G., White, R., Whiteman, C. D., and Wolfe, D.: The IMADA-AVER boundary layer experiment in the Mexico City area, Bull. Am. Meteorol. Soc., 79, 2497–2508, 1998.

Doran, J. C., Barnard, J. C., Arnott, W. P, Cary, R., Coulter, R., Fast, J. D., Kassianov, E. I, Kleinman, L., Laulainen, N. S, Martin, T, Paredes-Miranda, G. , Pekour, M. S., Shaw, W. J., Smith, D. F, Springston, S. R., and Yu, X.-Y.: The T1-T2 study: Evolution of aerosol properties downwind of Mexico City, Atmos. Chem. Phys., 7, 1585–1598, 2007a, http://www.atmos-chem-phys.net/7/1585/2007/.

Doran, J. C.: Corrigendum to: The T1–T2 study: evolution of aerosol properties downwind of Mexico City, Atmos. Chem. Phys., 7, 2197–2198, 2007, http://www.atmos-chem-phys.net/7/2197/2007/.

Doran, J. C., Fast, J. D., Barnard, J. C., Laskin, A., Desyaterik, Y., Gilles, M. K., and Hopkins, R. J.: Applications of Lagrangian dispersion modeling to the analysis of changes in the specific absorption of elemental carbon, Atmos. Chem. Phys., 8, 1377–1389, 2008, http://www.atmos-chem-phys.net/8/1377/2008/.

Dua, S. K., Hopke, P. K., and Raunemaa, T. Hygroscopicity of Diesel Aerosols, Water Air Soil Poll., 112, 247–257, 1999.

Dubovik, O., Holben, B. N., Kaufman, Y. J., Yamasoe, M., Smirnov, A., Tanre, D., and Slutsker, I.: Single scattering albedo of smoke retrieved from the sky radiance and solar transmittance measured from ground, J. Geophys. Res., 103, 31 903–31 923, 1998.

Eidels-Dubovoi, S.: Aerosol impacts on visible light extinction in the atmosphere of Mexico City, Science and the Total Environment, 287, 213–220, 2002.

Fast, J. D. and Zhong, S.: Meteorological factors associated with inhomogeneous ozone concentrations within the Mexico City basin, J. Geophys. Res., 103, 18 927–18 946, 1998.

Fast, J. D., de Foy, B., Acevedo Rosas, F., Caetano, E., Carmichael, G., Emmons, L., McKenna, D., Mena, M., Skamarock, W., Tie, X., Coulter, R. L., Barnard, J. C., Wiedinmyer, C., and Madronich, S.: A meteorological overview of the MILAGRO field campaigns, Atmos. Chem. Phys., 7, 2233–2257, 2007, http://www.atmos-chem-phys.net/7/2233/2007/.

Frederick, J. E. and Lubin, D.: The budget of biologically active radiation in the earth-atmosphere system, J. Geophys. Res., 93, 3825–3832, 1988.

Gaffney, J. S., Tanner, R. L., and Phillips, M.: Separating carbonaceous aerosol source terms using thermal evolution, carbon isotopic measurements, and C/N/S determinations, The Science and the Total Environment, 36, 53–60, 1984.

Gaffney, J. S. and Marley, N. A.: Uncertainties in climate change predictions: Aerosol effects, Atmos. Environ., 32, 2873–2874, 1998.

Gaffney, J. S., Marley, N. A., Cunningham, M. M., and Doskey, P. V.: Measurements of Peroxya-

cyl Nitrates (PANs) in Mexico City: Implications for Megacity Air Quality Impacts on Regional Scales, Atmos. Environ., 33, 5003–5012, 1999.
Gaffney, J. S., Marley, N. A., Drayton, P. J., Doskey, P. V., Kotamarthi, V. R., Cunningham, M. M., Baird, J. C., Dintaman, J., and Hart, H. L.: Field Observations of Regional and Urban Impacts on NO_2, Ozone, UV-B, and Nitrate Radical Production Rates: Nocturnal Urban Plumes and Regional Smoke Effects, Atmos. Environ., 36, 825–833, 2002.
Gaffney, J. S. and Marley, N. A.: The Importance of the Chemical and Physical Properties of Aerosols in Determining Their Transport and Residence Times in the Troposphere, Chapter 14, in: Urban Aerosols and Their Impacts: Lessons Learned from the World Trade Center Tragedy, edited by: Gaffney, J. S. and Marley, N. A., ACS Symposium Book 919, Oxford University Press, 286–300, 2005.
Gaffney, J. S., Marley, N. A., Tackett, M., Sturchio, N., Heraty, L., Martinez, N. Hardy, K., and Guilderson, T.: Biogenic Carbon Dominance Based on $^{13}C/^{12}C$ and ^{14}C Measurements of Total Carbon at T-0 and T-1 Sites during MILAGRO. 88th National Meeting of the American Meteorological Society. Tenth Conference on Atmospheric Chemistry, Conference Proceedings Volume, Paper J1.1, 5 pp. http://ams.confex.com/ams/pdfpapers/131852.pdf, 2008.
Granger, R. G., Basher, R. E., and McKenzie, R. L.: UV-B Robertson-Berger meter characterization and field calibration, Appl. Optics, 32, 343–349, 1993.
Hand, J. L., Kreidenweis, S. M., Slusser, J., and Scott, G.: Comparison of aerosol optical properties derived from Sun photometry to estimates inferred from surface measurements in Big Bend National Park, Texas, Atmos. Environ. 38, 6813–6821, 2004.
Hitzenberger, R. and Puxbaum, H.: Comparisons of the measured and calculated specific absorption coefficients for urban aerosol samples in Vienna, Aerosol Sci. Technol. 18, 323–345, 1993.
Hoffer, A., Gelencer, A., Guyon, P., Kiss, G., Schmid, O., Frank, G. P., Artaxo, P., and Andreae, M. O.: Optical properties of humic-like substances (HULIS) in biomass-burning aerosols, Atmos. Chem. Phys., 6, 3563–3570, 2006, http://www.atmos-chem-phys.net/6/3563/2006/.
Horvath, H., Catalan, L., and Trier, A.: A study of the aerosol of Santiago De Chile III: Light absorbing measurements, Atmos. Environ., 31, 3737–3744, 1997.
Jacobson, M. Z.: Global direct radiative forcing due to multicomponent anthropogenic and natural aerosols, J. Geophys. Res., 106, 1551–1568, 2001.
Jacobson, M. Z.: Control of fossil fuel particulate black carbon and organic matter, possibly the most effective method of slowing global warming, J. Geophys. Res., 107,

doi:10.1029/2001JD001376, 2002.
Jacobson, M. Z.: Climate response of fossil fuel and biofuel soot, accounting for soot's feedback to snow and sea ice albedo and emissivity. J. Geophys. Res., 109, D21201, doi:10.1029/2004JD004945, 2004.
Kirchstetter, T. W., Novakov, T., and Hobbs, P. V.: Evidence that the spectral dependence of light absorption by aerosols is affected by organic carbon, J. Geophys. Res., 109, D21208, doi:10.1029/2004JD004999, 2004.
Lenoble, J. and Brogniez, C.: Information on stratospheric aerosol characteristics contained in the SAGE satellite multiwavelength extinction measurements, Appl. Optics, 24, 1054–1063, 1985.
Marley, N. A., Gaffney, J. S., Drayton, P. J., Cunningham, M. M., Orlandini, K. A., and Paode, R.: Measurement of 210Pb, 210Po, and 210Bi in size-fractionated atmospheric aerosols: An estimate of fine-aerosol residence times, Aerosol Sci. Technol., 32, 569–583, 2000.
Marley, N. A. and Gaffney, J. S.: The Impact of Rain Events on Aerosol Optical Properties: Mexico City 2003 and 2006, EOS Transactions AGU, 88, (23), Joint Assembly Supplement, Abstract A41E-03, 2007.
McKinlay, A. and Diffy, B. L.: A reference action spectrum for ultraviolet induced erythema in human skin, in: Human exposure to ultraviolet radiation: Risks and Regulations, edited by: Passchler, W. R. and Bosnajokovic, B. F. M., Elsevier Science Publishers, Amsterdam, 83–87, 1987.
Molina, L. T. and Molina, M. J.: Air quality impacts: Local and global concern. Chapter 1, in: Air quality in the Mexico Megacity, An integrated assessment, edited by: Molina, L. T. and Molina, M. J., Kluwer Academic, Netherlands, 2002.
O'Niell, N. and Royer, A.: Extraction of bimodal aerosol-size distribution radii from spectral and angular slope (Angstrom) coefficients, Appl. Optics, 32, 1642–1645, 1993.
Patterson, E. M. and McMahon, C. K.: Absorption characteristics of forest fire particulate matter, Atmos. Environ., 18, 2541–2551, 1984.
Petzold, A., Schloesser, H., Sheridan, P. J., Arnott, W. P., Ogren, J. A., and Virkkula, A.: Evaluation of Multiangle Absorption Photometry for measuring aerosol light absorption, Aerosol Sci. Technol, 39, 40–51, 2005.
Pósfai, M., Anderson, J. R., Buseck, P. R., and Sievering, H.: Soot and sulfate aerosol particles in the remote marine troposphere, J. Geophys. Res., 104, 21 685–21 683, 1999.
Raga, G. B., Castro, T., and Baumgardner, D.: The impact of megacity pollution on local climate

and implications for the regional environment: Mexico City, Atmos. Environ., 35, 1805–1811, 2001a.
Raga, G. B., Baumgardner, D., Castro, T., Martìnez-Arroyo, A., and Navarro-González, R.: Mexico City air quality: a qualitative review of gas and aerosol measurements (1960–2000), Atmos. Environ., 35, 4041–4058, 2001b.
Ramanathan, V., Crutzen, P. J., Kiehl, J. T., and Rosenfeld, D.: Aerosols, climate, and the hydrological cycle, Science 7, 2119–2124, 2001.
Ramanathan, V., Chung, C., Kim, D., Bettge, T., Buja, L., Kiel, J. T., Washington, W. M., Fu, Q., Sikka, D. R., and Wild, M.: Atmospheric brown clouds: Impacts on South Asian climate and hydrological cycle, Proceedings of the National Academy of Science, USA 102, 5326–5333, 2005.
Salcedo, D., Onasch, T. B., Dzepina, K., Canagaratna, M. R., Zhang, J. Q., Huffman, A., DeCarlo, P. F., Jayne, J. T., Mortimer, P., Worsnop, D. R., Kolb, C. E., Johnson, K. S., Zuberi, B., Marr, L. C., Volkamer, R., Molina, L. T., Molina, M. J., Cardenas, B., Bernabé R. M., Márquez, C., Gaffney, J. S., Marley, N. A., Laskin, A., Shutthanandan, V., Xie, Y., Brune, W., Lesher, R., Shirley, T., and Jimenez, J. L.: Characterization of ambient aerosols in Mexico City during the MCMA-2003 campaign with Aerosol Mass Spectrometry: results from the CENICA Supersite, Atmos. Chem. Phys., 6, 925–946, 2006, http://www.atmos-chem-phys.net/6/925/2006/.
Schwartz, S. E. and Buseck, P. R.: Absorbing phenomena, Science, 288, 989–990, 2000.
Schmid, O., Artaxo, P., Arnott, W. P., Chand, D., Gatti, L. V., Frank, G. P., Hoffer, A., Schnaiter, M., and Andrae, M. O.: Spectral light absorption by ambient aerosols influenced by biomass burning in the Amazon Basin. I: Comparison and field calibration of absorption measurement techniques, Atmos. Chem. Phys., 6, 3443–3462, 2006, http://www.atmos-chem-phys.net/6/3443/2006/.
Schnaiter, M., Linke, C., Möhler, O., Naumann, K.-H., Saathoff, H., Wagner, R., Schurath, U., and Wehner, B.: Absorption amplification of black carbon internally mixed with secondary organic aerosol, J. Geophys. Res., 110, doi:10.1029/2005JD006046, 2005.
Swap, R. J., Annegarn, H. J., Suttes, J. T., King, M. D., Platnick, S., Privette, J. L., and Scholes, R. J.: Africa burning: A thematic analysis of the Southern African Regional Science Initiative (SAFARI 2000), J. Geophys. Res., 108, D13, 8465, doi:10.1029/2003JD003747, 2003.
Tanner, R. L., Gaffney, J. S., and Phillips, M. F.: Determination of Organic and Elemental Carbon in Atmospheric Aerosol Samples by Thermal Evolution, Anal. Chem., 54, 1627–1630, 1982.

UNEP/WHO (United Nations Environmental Program/World Health Organization): Urban Air Pollution in Megacities of the World, Blackwell Publisher, Oxford, 1992.

Whiteman, C. D., Zhong, S., Bian, X., Fast, J. D., and Doran, J. C.: Boundary layer evolution and regional scale diurnal circulations over the Mexican plateau, J. Geophys. Res., 105, 10 081–10 102, 2000.

Williams, J., de Reus, M., Krejci, R., Fischer, H., and Ström, J.: Application of the variability-size relationship to atmospheric aerosol studies: estimating aerosol lifetimes and ages, Atmos. Chem. Phys., 2, 133–145, 2002, http://www.atmos-chem-phys.net/2/133/2002/.

ACPD

8, 12625–12663, 2008

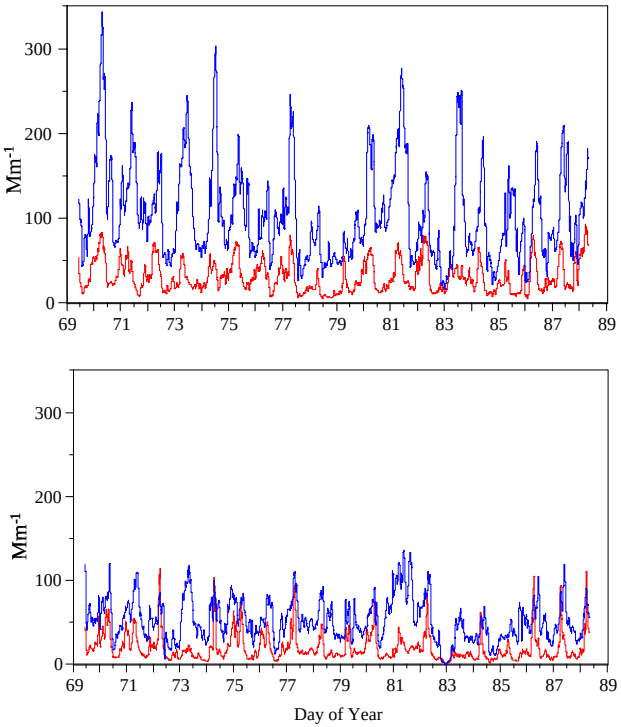

Fig. 1. Measurements of fine (<1 micron) aerosol absorption (red) and scattering (blue) obtained at sites T0 (top) and T1 (bottom) from 10 March (day 69) to 29 March, (day 88) 2006 during the MILAGRO field campaign.

ACPD
8, 12625–12663, 2008

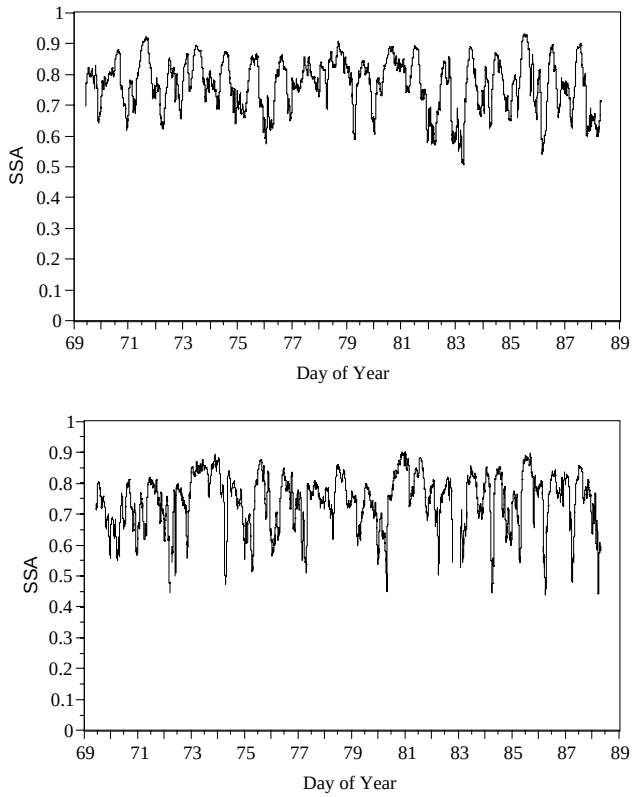

Fig. 2. Aerosol single scattering albedo (SSA) determined at site T0 (top) and T1 (bottom) from 10 March (day 69) to 29 March, (day 88) 2006 during the MILAGRO field campaign.

ACPD
8, 12625–12663, 2008

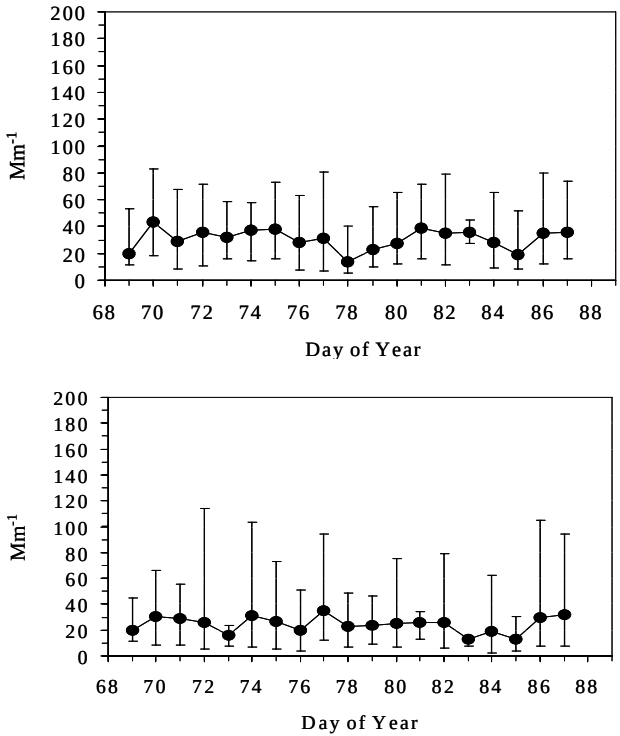

Fig. 3. Daily aerosol absorption averaged from 06:00–18:00 LST and absorption ranges measured at sites T0 (top) and T1 (bottom) from March 10 (day 69) to 29 March, (day 88) 2006 during the MILAGRO field campaign.

ACPD
8, 12625–12663, 2008

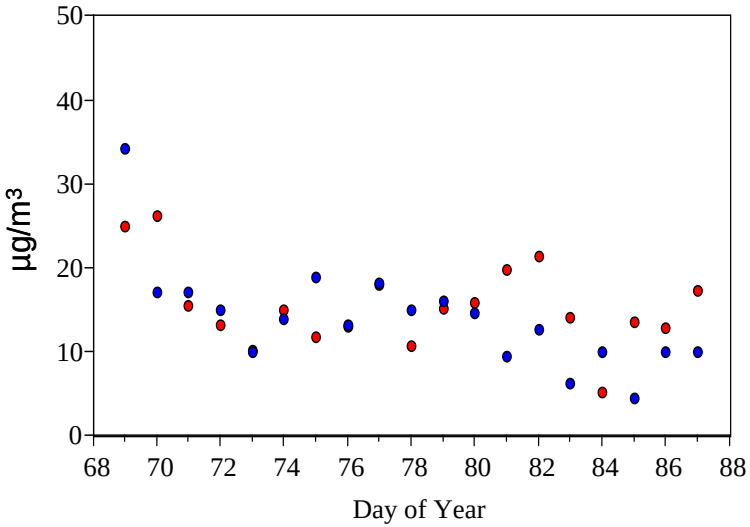

Fig. 4. Total carbon concentrations measured on fine (<0.2 micron) aerosol samples collected from 05:30–17:30 at site T0 (red) and T1 (blue) from 10 March (day 69) to 29 March, (day 88) 2006 during the MILAGRO field campaign.

ACPD
8, 12625–12663, 2008

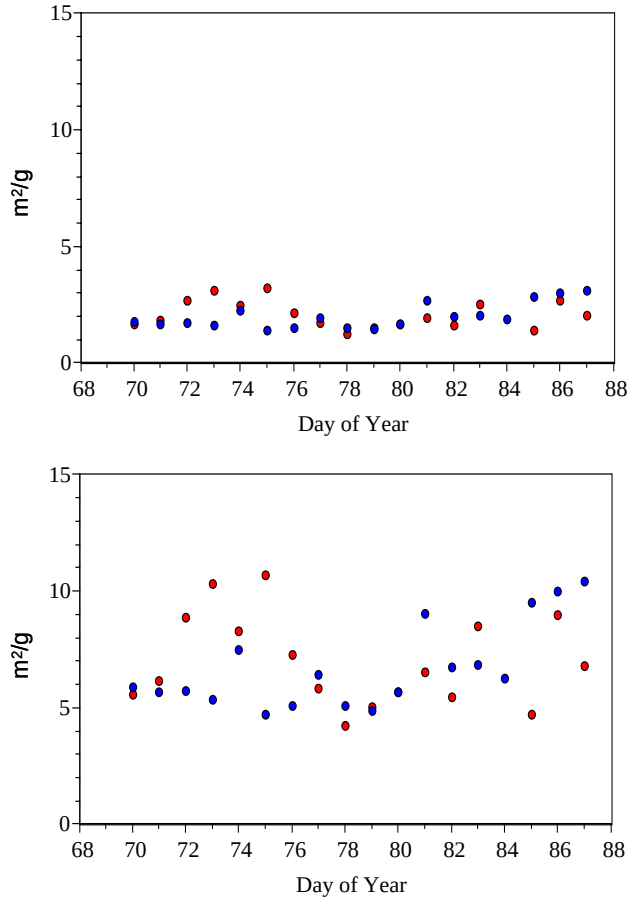

Fig. 5. Daily average mass absorption coefficient calculated for total carbon (top) and black carbon (bottom) at site T0 (red) and T1 (blue) from 10 March (day 69) to 29 March, (day 88) 2006 during the MILAGRO field campaign.

ACPD
8, 12625–12663, 2008

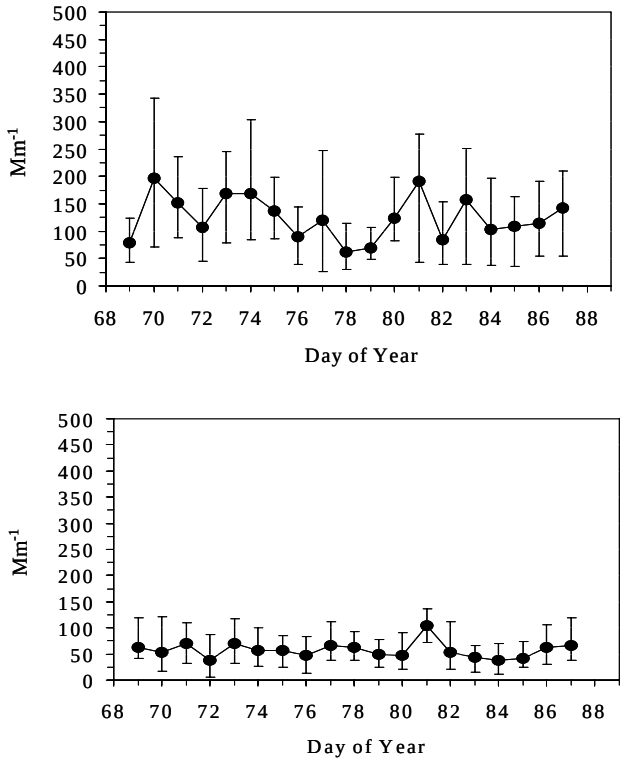

Fig. 6. Daily aerosol scattering averaged from 06:00–18:00 LST and scattering ranges measured at sites T0 (top) and T1 (bottom) from 10 March (day 69) to 29 March, (day 88) 2006 during the MILAGRO field campaign.

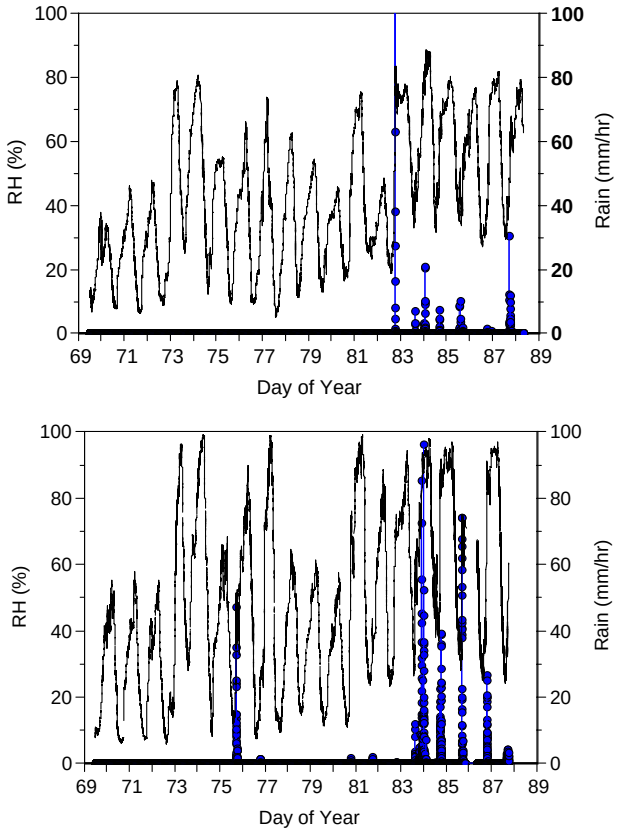

Fig. 7. Relative humidity and rain intensity (blue) measured at sites T0 (top) and T1 (bottom) from 10 March (day 69) to 29 March (day 88) 2006 during the MILAGRO field campaign.

ACPD
8, 12625–12663, 2008

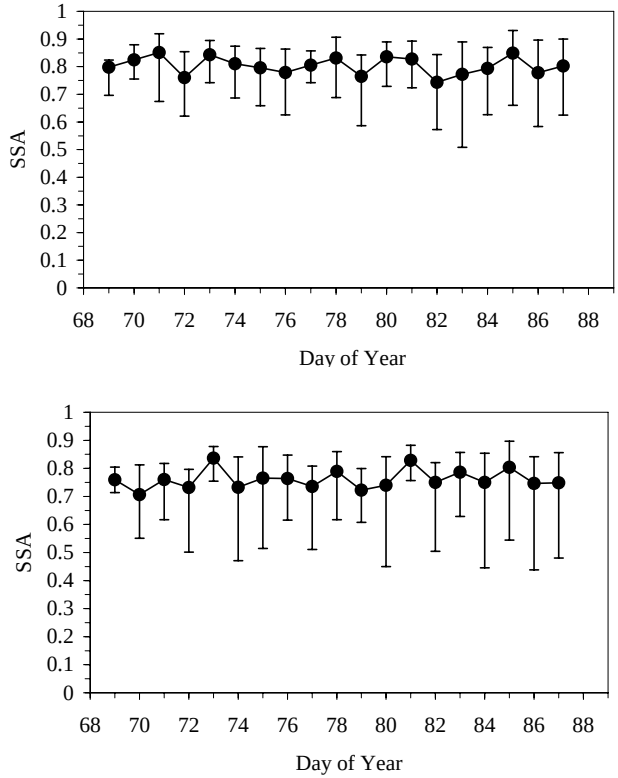

Fig. 8. Daily aerosol single scattering albedo (SSA) averaged from 06:00–18:00 LST and SSA ranges measured at sites T0 (top) and T1 (bottom) from 10 March (day 69) to 29 March, (day 88) 2006 during the MILAGRO field campaign.

ACPD
8, 12625–12663, 2008

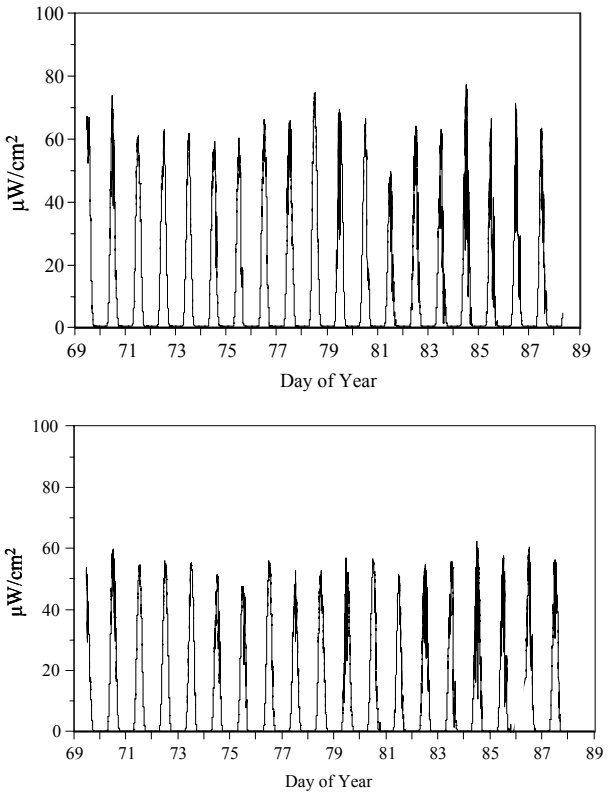

Fig. 9. Broadband UVB measured at sites T0 (top) and T1 (bottom) from 10 March (day 69) to 29 March, (day 88) 2006 during the MILAGRO field campaign.

ACPD
8, 12625–12663, 2008

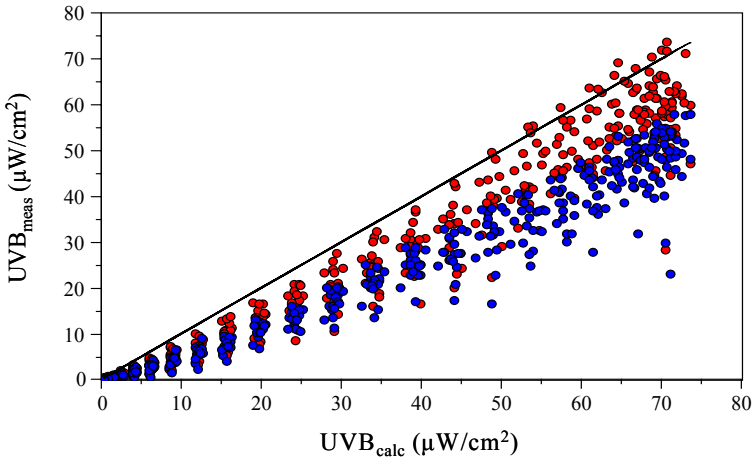

Fig. 10. Broadband UVB measured at sites T0 (red) and T1 (blue) compared to calculated clear sky UVB on days without rain events during the MILAGRO field campaign.

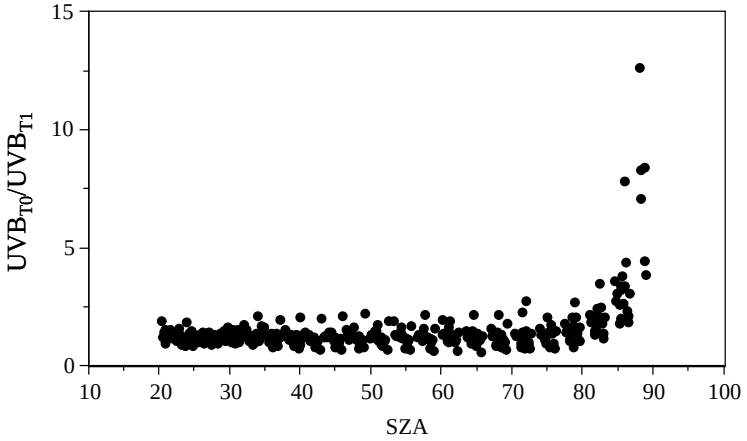

Fig. 11. Ratio of broadband UVB measured at sites T0 and T1 on days without rain events as a function of solar zenith angle (SZA) during the MILAGRO field campaign.

ACPD
8, 12625–12663, 2008